II International Conference - Industrial Engineering And Environmental Protection (IIZS 2012)

UNIVERSITY OF NOVI SAD
Technical faculty "Mihajlo Pupin"
Zrenjanin, Republic of Serbia

Industrial Engineering and Environmental Protection

IIZS conference 2012

PROCEEDINGS

II International Conference - Industrial Engineering And Environmental Protection (IIZS 2012)

Zrenjanin Town Hall
Zrenjanin, 31st October 2012.

University of Novi Sad
Technical faculty "Mihajlo Pupin"
Zrenjanin, Republic of Serbia

II International Conference Industrial Engineering and Environmental Protection (IIZS 2012)

Proceedings

Zrenjanin, 31st October 2012.

II International Conference - Industrial Engineering and Environmental Protection (IIZS 2012)

Organizer of the Conference:
Technical faculty "Mihajlo Pupin", Zrenjanin, University of Novi Sad, Republic of Serbia

Reviewers:
Ph.D James G. Speight, CD&W Inc., Laramie,Wyoming, USA
Ph.D Slawomir Kurpaska, Professor, University of Agriculture in Krakow Institute of Agricultural, Engineering and Informatics
Ph.D Dragiša Tolmač, Professor, Technical faculty "Mihajlo Pupin", Zrenjanin, Republic of Serbia
Ph.D Miroslav Lambić, Professor, Technical faculty "Mihajlo Pupin", Zrenjanin, Republic of Serbia

Publisher:
Technical faculty "Mihajlo Pupin", Zrenjanin, University of Novi Sad

For publisher:
Ph.D Milan Pavlović, Dean of Technical faculty "Mihajlo Pupin", Zrenjanin

Technical treatment:
Ph.D Eleonora Desnica, Technical faculty "Mihajlo Pupin", Zrenjanin, Republic of Serbia
Ph.D Ljiljana Radovanović, Technical faculty "Mihajlo Pupin", Zrenjanin, Republic of Serbia
MSc. Jasmina Pekez, Technical faculty "Mihajlo Pupin", Zrenjanin, Republic of Serbia

Design:
MSc. Stanislava Sinđelić, Technical faculty "Mihajlo Pupin", Zrenjanin, Republic of Serbia

Lecturer:
MSc. Dragica Ivin, Technical faculty "Mihajlo Pupin", Zrenjanin, Republic of Serbia

Printed by: Printig office »Diginet«, Zrenjanin
Circulation: 100
ISBN: 978-86-7672-184-9

CIP – Каталогизација у публикацији
Библиотека Матице српске, Нови Сад

502/504 (082)

INTERNATIONAL Conference Industrial engineering and Environmental Protection (2; 2012; Zrenjanin)
Proceedings / II International Conference Industrial Engineering and Environmental Protection (IIZS 2012), Zrenjanin, 31st October 2012; [organizer of the Symposium] Technical faculty "Mihajlo Pupin", Zrenjanin . – Zrenjanin: Technical faculty "Mihajlo Pupin", 2012 (Zrenjanin: Diginet) – 490 str. : ilustr.; 30 cm.

Tiraž 100. – Str. 5: Introduction/ Dragiša Tolmač
Bibliografija uz svaki rad.

ISBN 978-86-7672-184-9
1. Technical faculty "Mihajlo Pupin" (Zrenjanin). – I. IIZS conference (2; 2012; Zrenjanin) v. International Conference Industrial Engineering and Environmental Protection (2; 2012: Zrenjanin)

a) Животна средина – Заштита - Зборници
COBISS. SR-ID 274556935

Scientific Committee:

Ph.D Dragiša Tolmač, President, Technical Faculty "Mihajlo Pupin", Zrenjanin, Serbia

Ph.D James G. Speight, CD&W Inc., Laramie,Wyoming, USA

Ph.D Slawomir Kurpaska, Faculty of Agric. Engineering, Agricultural University, Krakow

Ph.D Miroslav Lambić, Technical Faculty "Mihajlo Pupin", Zrenjanin, Serbia

Ph.D Uroš Karadžić, Mechanical Engineering, Podgorica, Montenegro

Ph.D Dimitar G. Petrov, Technical University, Sofia, Bulgaria

Ph.D Živoslav Adamović, Technical Faculty "Mihajlo Pupin", Zrenjanin, Serbia

Ph.D José L. Lage, Department of Mechanical Engineering, Southern Methodist University, Dallas, USA

Ph. D Yoncho Pelovsky, University of chemical Technology and Metalurgy, Educational centers, Center of ecology, Sofia, Bulgaria

Ph.D Valentina Emilia Balas, „Aurel Vlaicu" University of Arad, Faculty of Engineering, Arad, Romania

Ph.D Mirko Soković, Mechanical Engineering, Ljubljana, Slovenia

Ph.D Džafer Kudumović, Faculty of Mechanical Engineering, Bosnia and Herzegovina

Ph.D Mitko Mitkovski, Technical University Sofia - Plovdiv, Bulgaria

Ph.D Slavica Prvulović, Technical Faculty "Mihajlo Pupin", Zrenjanin, Serbia

Ph.D Vincenc Butala, University of Ljubljana, Slovenia

Ph.D Slobodan Stojadinović, Technical Faculty "Mihajlo Pupin", Zrenjanin, Serbia

Ph.D Zoran Markov, Faculty of Mechanical Engineering, Skopje, Macedonia

Ph.D Zvonko Sajfert, Technical Faculty "Mihajlo Pupin", Zrenjanin, Serbia

Ph.D Nicolae Farbas, National R & D Institute of Welding and Material Testing

Ph.D Bojan Podgornik, Faculty of Mechanical Engineering, University of Ljubljana, Slovenia

Ph.D Ljubica Diković, High business technical school of Užice, Serbia

Ph.D Eleonora Desnica, Technical Faculty "Mihajlo Pupin", Zrenjanin, Serbia

Ph.D Goran Vujić, FTN - Faculty of Technical Sciences, Novi Sad, Serbia

Ph.D Miroslav Stanojević, Faculty of Mechanical Engineering, Belgrade, Serbia

Ph.D Jasmina Radosavljević, Faculty of Occupational Safety, Niš, Serbia

Ph.D Ivo Čala, Polytechnic of Zagreb, Croatia

Ph.D Mladen Stojiljković, Faculty of Mechanical Engineering, Niš

Ph.D Miodrag Stojiljković, Faculty of Mechanical Engineering, Niš

Ph.D Radmila Stikić, Faculty of Agriculture, Zemun, Serbia

Ph.D Snežana Dragićević, Technical Faculty, Čačak, Serbia

Ph.D Aleksandar Petrović, Faculty of Mechanical Engineering, Belgrade, Serbia

Ph.D Radivoj Topić, Faculty of Mechanical Engineering, Belgrade, Serbia.

Organizing Committee:

Ph.D Dragiša Tolmač, Technical faculty “Mihajlo Pupin”, Zrenjanin, Republic of Serbia
Ph.D Živoslav Adamović, Technical faculty “Mihajlo Pupin”, Zrenjanin, Republic of Serbia
Ph.D Miroslav Lambić, Technical faculty “Mihajlo Pupin”, Zrenjanin, Republic of Serbia
Ph.D Slobodan Stojadinović, Technical faculty “Mihajlo Pupin”, Zrenjanin, Republic of Serbia
Ph.D Slavica Prvulović, Technical faculty “Mihajlo Pupin”, Zrenjanin, Republic of Serbia
Ph.D Eleonora Desnica, Technical faculty “Mihajlo Pupin”, Zrenjanin, Republic of Serbia
Ph.D Ljiljana Radovanović, Technical faculty “Mihajlo Pupin”, Zrenjanin, Republic of Serbia
MSc. Jasmina Pekez, Technical faculty “Mihajlo Pupin”, Zrenjanin, Republic of Serbia

CORROSION BEHAVIOUR OF AN Al-Zn-Mg-Cu ALLOY AFTER DIFFERENT HEAT TREATMENTS

Ana Alil[1], Bore Jegdić, Biljana Bobić, Marko Ristić
[1]Institute Goša, Milana Rakića 35, Belgrade, Serbia
e-mail: ana.alil@institutgosa.rs

Abstract: The variation of factors such as the amount of alloying elements in solid solution, thermal and thermo-mechanical treatments changes the corrosion tendency in the Al-Zn-Mg-Cu alloy. The measurements of electrical conductivity enabled the estimation of the structural state of the alloy, i.e. the type and the degree of precipitation.The corrosion behaviour was examined through three electrochemical methods($E_{corr.}$, polarization measurements, EIS).The measurement of corrosion potentials ($E_{corr.}$) gave information about the distribution of the alloying elements between the solid solution and the precipitation phases. The polarization measurements have shown a more positive value of pitting potential ($E_{pit.}$) and a greater resistance to corrosionfor the two-step aged alloy. The electrochemical impedance spectroscopy (EIS) has also shown that the two-step aged alloy has better corrosion propertiescompared to the one-step aged alloy.The fracture mechanics (FM) method wasused for SCC testing and hasshown that the alloy after two-step precipitation hardening is significantly more resistant to SCC. The obtained results enable a greaterinsight into the effects of both heat treatment and alloying elements, primarily copper, on the corrosion resistance of the alloy.
Key words: aluminium alloys, electrochemical methods, fracture mechanics,stress corrosion cracking

INTRODUCTION

Even the Al-Zn-Mg-Cu alloys have maximum strength; they are prone to localized types of corrosion and also to stress corrosion cracking (SCC). However, the tendency of these alloys to corrode changes depending on the content of alloying elements as well as on mechanical, thermal and thermo-mechanical treatments [1-4]. The precipitation hardening of the 7000 series Al-alloys takes place through the segregation of GP zones that are transformed through the intermediate η' phase into the equilibrium phase $MgZn_2$[5-8]. The maximum strength is achieved where there is a mixture of GP zones and η' precipitatesin the structure. But, in the state of maximum strength the alloy is prone to SCC. Stress corrosion cracking is a time-dependent process that occurs under the influence of residual or imposed tensile stress and specific corrosion environment. Localized corrosion (intergranular, pitting) usually proceeds to the SCC. For SCC to occur, the following conditions have to be fulfilled: the alloy is prone to SCC, the alloy is in a specific corrosion environment and the value of tensile stress is higher than the threshold value [2]. According to fracture mechanics (FM), the third condition is defined so that the coefficient of the stress intensity on the crack tip K_I is higher than some critical value K_{ISCC} [3]. The addition of copper in these alloys increase the volume fraction of the hardening precipitates. It was found that copper is incorporated in the GP zones, making them more stable even at higher temperatures [5, 9, 10]. In addition, copper atoms replace zinc atoms in the hardening precipitate η' ($MgZn_2$), particularly at temperatures above 150 °C [10], making the precipitate nobler. All this provide conditions for the increased resistance of these alloys to SCC. The electrochemical and corrosion characteristics of the alloy in the state after one and after a two-stage aging process were investigated in this paper.

EXPERIMENTAL PART

Material

The chemical composition of the tested alloy is given in Table 1.

Table 1. Chemical composition of the Al-Zn-Mg-Cu alloy (wt. %):

Zn	Mg	Cu	Mn	Cr	Zr	Al
7.2	2.15	1.46	0.28	0.16	0.12	Rest

The heat treatment of the samples was performed according to two different regimes: 1) homogenization annealing at 460°C/1h, quenching in water at room temperature, then precipitation hardening at 120°C/24h (one-stage aging, indicated in this paper with TA), 2) homogenization annealing at 460°C/1h, quenching in water at room temperature, precipitation hardening at 100°C/5h, and then at 160°C/5h (two-stage aging, indicated in this paper with TB).

Measurements of electrical resistivity

The method of measurement is described in ASTM B193 standard. Electrical resistivity was measured on the TA and TB samples by a microohmmeter in accordance with the manufacturer's instructions. The value of the measured electrical resistivity (ρ) was recalculated into electrical conductivity (($\chi=1/\rho$), as well as into the IACS% factor, using the equation:

$$IACS = \frac{\chi}{\chi_{Cu}} \cdot 100\% \qquad (1)$$

where χ is the value of the electrical conductivity of the tested alloy and χ_{Cu} is the electrical conductivity of pure copper (58.34 MS m^{-1}).

Corrosion potential measurements

Corrosion potential measurements were performed on the TA and TB samples. The samples (working electrodes) were degreased by ethanol and then placed in the electrochemical cell with a saturated calomel electrode (SCE) as a reference electrode. The measurements were performed in the 3.5 wt. % NaCl solution. The changes in the corrosion potential were monitored at room temperature, in the presence of atmospheric air, during 60 min.

Polarisation measurements

The cathodic and anodic polarization curves of the TA and TB samples were obtained using the GAMRY Reference 600 Potentiostat / Galvanostat / ZRA in deaerated 3.5 wt. % NaCl at room temperature. A three-electrode cell arrangement was used in the experiments. The working electrode was the sample, placed in a special holder, whilethe counter electrode was a platinum mesh with a surface area considerably greater than that of the working electrode. The reference electrode was the SCE. A potential sweep rate of 0.5 mV s^{-1} was applied after the constant open circuit potential was established (up to 30 min).

Electrochemical impedance spectroscopy measurements

For electrochemical impedance spectroscopy (EIS) measurements, the TA and TB samples were exposed to 3.5 wt. % NaCl for 48 h, anda three-electrode cell arrangement was used as in the polarization measurements. The EIS data were obtained at the open-circuit potential using the GAMRY Reference 600 potentiostat / galvanostat / ZRA. The impedance measurements were carried out over a frequency range of 100 kHz to 10 mHz using the 10 mV amplitude of sinusoidal voltage. The impedance spectra were analyzed using the GAMRY Elchem Analyst fitting procedure.

Fracture mechanics (FM) method

A bolt-loaded double-cantilever-beam (DCB) test specimen was chosen for testing SCC by the FM methodology. The samples were cut in the S-L orientation since aluminium alloys are most sensitive to SCC at this orientation. The starting value of the K_{I0} was calculated on the basis of the measured value of the crack length (a), the sample half-height (H) and the given size of the crack opening on the line of the load (V_Y), according to the following equation [ISO 7539-6]:

$$K_{I0} = \frac{E \cdot V_Y \cdot H \cdot \sqrt{3H\left(a+0{,}6H\right)^2 + H^3}}{4\left[\left(a+0{,}6H\right)^3 + H^2 a\right]} \qquad (2)$$

The starting crack was formed mechanically on the sample and the crack length was precisely measured. The increase of the crack length was measured microscopically in the next 150 days. The diagram of time dependence of the crack length is used for calculating and drawing the diagram of the crack growth rate dependence on the K_I. The real value of the stress intensity and the real value of the stress intensity when the crack practically stops, K_{ISCC}, were calculated (equ.2). In addition, SCC tests at different temperatures were done in a 3.5 wt. % NaCl solution. The length of the crack was measured during the time and the $v_{pl}$was calculated for every chosen temperature.

RESULTS AND DISCUSSION

The tested Al-Zn-Mg-Cu alloy, aged according to the TA and TB regimes, is characterized with an appropriate structure, mechanical properties, corrosion resistance, electrical conductivity and electrochemical properties. Based on these indicators, the tendency of the alloy to SCC and to localized corrosion was evaluated.

Electrical conductivity

The electrical resistivity and the recalculated values of electrical conductivity and the IACS% factor for TA and TB state of the tested aluminium alloy are shown in Table 2.

Table 2. Electrical resistivity and the recalculated values of electrical conductivity and the IACS factor after homogenization annealing (T0), one-stage (TA) and two-stage (TB) aging.

Thermal State	ρ (nΩ m)	χ (MS m-1)	IACS (%)
T0	5.82	17.20	29.65
TA	5.30	18.88	32.56
TB	4.75	21.06	36.71

The obtained results have shown that the TB sample has larger conductivity than the TA sample and the T0sample. A supersaturated solid solution with a high concentration of vacancies was obtained after quenching. Fields of elastic strains around vacancies cause dissipation of electrons, so lower values of conductivity are obtained. During aging, the clusters of zinc are formed at first, followed by the GP zones which grow gradually and transform themselves into the half-coherent phase η'. Elastic strains around the GP zones and the η' phase caused more electron dissipation. With appearance of the stabile η phase during two-stage aging, elastic strains decrease, and the alloy conductivity increases.

Electrochemical properties

In the test solution, at a constant temperature, the corrosion potential value of the tested aluminium alloy depends on the content of the alloying elements in the solid solution [11]. The results presented in Fig.1 show that the corrosion potential has a higher value after two-stage (TB), than after one-stage

aging (TA). This can be related to the kinetics of the precipitation hardening. The alloy in the TA thermal state has a larger concentration of zinc (more negative) in the solid solution, which results in a more negative value of the corrosion potential (E_{corr} = -795 mV). In the case of the TB thermal state (partially over-aged state), the enlargement of the straightening precipitates occurs at the expense of impoverishment of the solid solution in zinc, magnesium and copper. In this case, the solid solution has a more positive corrosion potential (E_{corr} = -775 mV) due to depletion in zinc and magnesium. The formed precipitates after two-stage aging have become more electrically positive than the precipitates after one-stage aging. The atoms of aluminium and copper are incorporated in ($MgZn_2$), replacing to some extent the atoms of zinc and forming $Mg(AlCuZn)_2$.

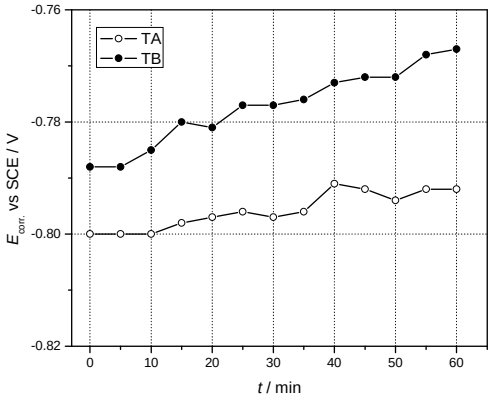

Figure 1. Time dependence of E_{corr} of the aluminium alloy in the TA and TB state.

The polarization curves of aluminium alloy after one-stage and two-stage aging are shown in Fig.2. It can be seen that the sample TB has a more positive value of the pitting potential (E_{pit} = -775 mV) with regard to the sample TA (E_{pit} = -800 mV). Also, the value of the corrosion current density for the alloy in the TB state is lower than for the alloy in the TA state, whereas the anodic and cathodic curves are shifted to the lower current density for the alloy in the TB state.

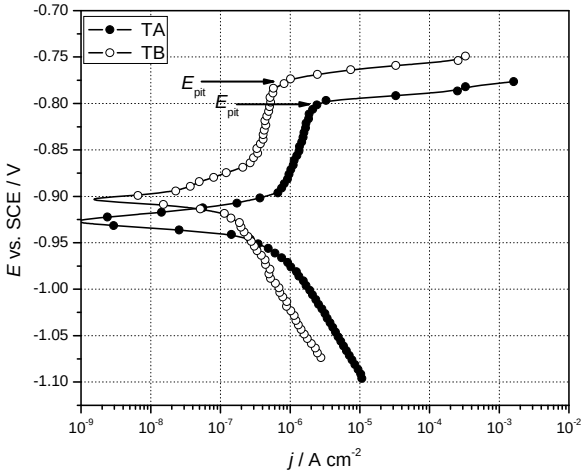

Figure 2. Polarisation diagrams of the aluminium alloy in the TA and TB states in deaerated 3.5 % NaCl at room temperature.

In the 7000 series alloys, pitting occurs due to the local dissolution of the matrix or to the dissolution of intermetallic compounds [13]. The explanation for the alloy's behaviour after two-stage aging lies in the fact that the difference in the electrode potentials between the intermetallic compounds and the solid solution has been decreased as well as the electrode potential difference between the precipitates and the solid solution. It was noticed that two pitting potentials exist,with the appearance of the second pitting potential at current densities higher than 1 mA cm^{-2} [12, 13]. The Nyquist complex plane plots of aluminium alloys in TA and TB state obtained by the EIS measurements are shown in Fig.3. The alloys in both thermal states show almost ideal Nyquist semicircle after one hour in 3.5 wt. % NaCl. The polarization resistance, R_p, of the alloy in the TA state is lower (which corresponds to a

higher corrosion rate) with regard to R_p of the TB state (Table 3). After 24 h, a so-called Warburg's diffusion tail has appeared on the Nyquist diagram for the TA sample. A similar diffusion tail has appeared for the TB sample, also, after 48 h. However, the value of R_p was higher for the TB sample that corresponds to a lower corrosion rate.At the surface of the tested samples a layer of dark corrosion products has been formed, probably consisting of $Al(OH)_3$. A significant increase in the double layer capacitance capacitance (C_{dl}) and a decrease in the polarization resistance (R_p) with time indicate lower corrosion characteristics of the alloy after one-stage aging (Table 3).

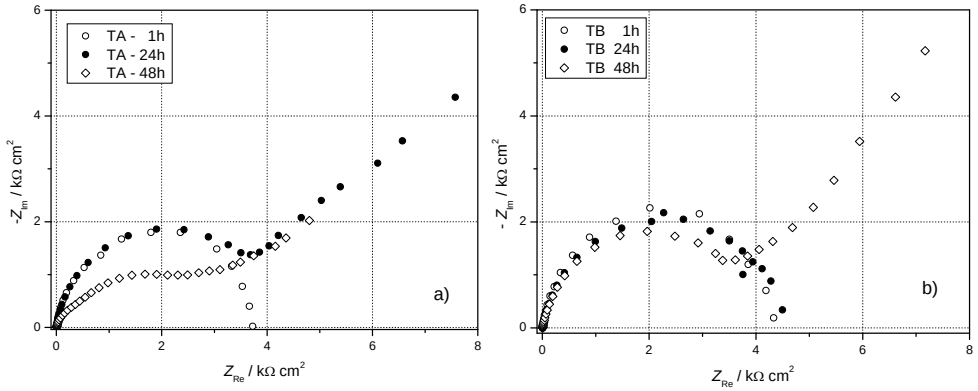

Figure 3. Nyquist plots of the aluminium alloys in 3.5 wt.% NaCl at room temperature after a) one-stage aging (TA), b) two-stage aging (TB).

Table 3. The values of corrosion potential, E_{corr}, double layer capacitance, C_{dl}, polarization resistance, R_p and pitting potential, E_{pit} after one-stage aging (TA) and two-stage aging (TB).

t (h)	Thermal State TA			
	E_{corr} (mV)	C_{dl} (μF cm^{-2})	R_p (kΩ cm^2)	E_{pit} (mV)
1	-795	12.5	3.86	-800
24	-775	22.7	4.18	-
48	-750	118.2	2.84	-
	Thermal State TB			
1	-770	7.9	4.33	-775
24	-755	28.7	4.56	-
48	-740	28.9	4.06	-

Fracture mechanics (FM) method

The main advantage of the FM method is getting quantitative data about alloy susceptibility to SCC (K_{ISCC}, $v = da/dt$). A diagram of dependence of the stress corrosion crack rate on the K_I is given in Fig.4. When the K_I is smaller than the K_{ISCC}, there is no growth of the stress corrosion crack or the growth rate is too small that can be neglected. In the first stadium (I), the crack growth rate strongly depends on the K_I. In the second stadium (II), the crack growth rate does not depend on the K_I. The influence of the alloy heat treatment is significant and it reflects in shifting the level of the second stadium to higher or lower values (Fig.4). In the third stadium (III), v increases fast until the critical value K_{IC} is reached, when it comes to a quasi-static fracture. It can be seen (Fig.4 and Table 4) that the alloy is more resistant to SCC after two-step aging (TB). The difference in SCC resistance is reflected on the v_{pl} value. The value of the v_{pl} is lower for more than one order of magnitude in the TB case. The maximum strength of the alloy (TA state) is obtained when GP zones and η' precipitates are present in a structure. Local plastic deformation at the tip of the stress corrosion crack causes mainly planar slipping when dislocations cut GP zones and smaller particles of the η' phase. It comes to the accumulation of dislocations at the grain boundaries at the crack tip, which causes increase in local stress, so that SCC starts at lower external stress [5,7].

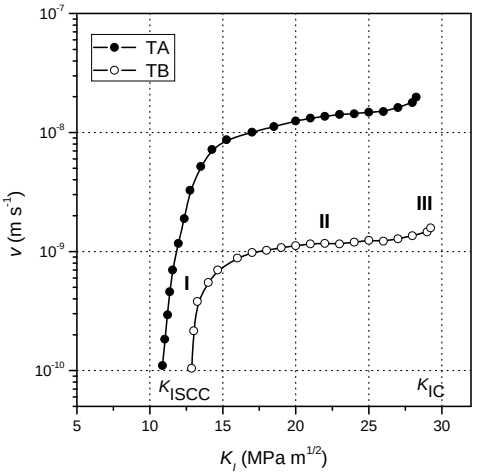

Figure 4. Influence of the heat treatment regime on the log v - $K_I$dependence.

Table 4. Results of the SCC testing by the FM method.

Therma l State	K_{I0} (MPa $m^{1/2}$)	K_{ISCC} (MPa $m^{1/2}$)	v_{pl} (m s-1)
TA	28.25	10.87	14.4 10^{-9}
TB	29.25	12.87	1.16 10^{-9}

In the TB case, a great number of GP zones is created in the first stage, at a lower temperature (100°C). The smaller particles (of the η' phase) precipitate on the GP zones during the second stage of aging (160°C) and then, they are partially transformed into the stable ηphase. In this case, the local plastic deformation at the crack tip is homogeneous (so-called turbulent slipping). Dislocations cannot succeed in cutting the particles of the stable ηphase and are uniformly distributed inside the grains. There is no local increase in stress at the grain boundaries and that creates favorable conditions for higher resistance to SCC [5, 7].

Addition of copper affects in the electrochemical characteristics of the alloy structural constituents. In the Al-Zn-Mg alloys, the ηphase precipitated on the grain boundary is anodic compared to the grain itself (which is covered with a passive film). These conditions are favourable for intergranular corrosion and SCC to occur. In the tested alloy, copper atoms enter into the solid solution and into the precipitates, making them nobler [9]. The precipitates on the grain boundaries are dissolved slower, and the cathodic reaction (hydrogen ion reduction) becomes more difficult [5, 9]. Copper has influence on mechanism of plastic deformation (slipping) and on electrochemical characteristics of the matrix and the precipitates. All this contributes to the increased SCC resistance.

The influence of the test solution temperature on the v_{pl} is shown in Figure 5. The exponential increase of the v_{pl} with the increase in temperature can be noticed, which is expressed by the following equation:

$$v = v_0 \exp(-E_a/RT) \qquad (3)$$

where$E_a$is the apparent activation energy of the process that controls the v_{pl}.

If the previous equation is logarithmed, a linear dependence between the logarithm of the v_{pl} and the reciprocal value of the temperature is gained.

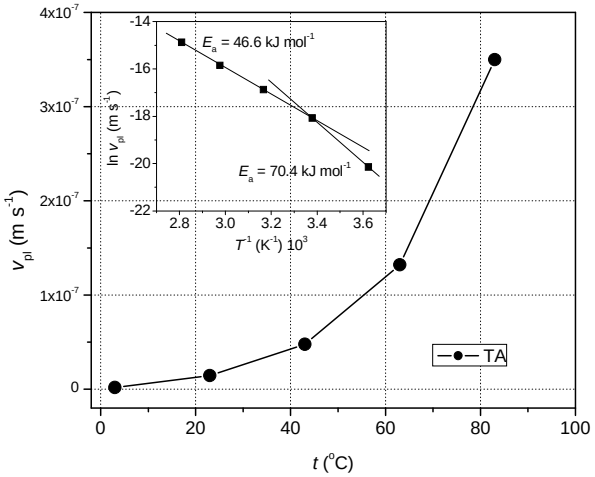

Figure 5. v_{pl}dependence of temperature during SCC testing (TA state).

The dependence of the v_{pl} on the reciprocal value of the temperature is shown in the insert in Fig.5. The apparent activation energy of the process that controls the v_{pl} is obtainedfrom the slope. There are two values of the apparent activation energy. One value (E_a = 46.6 kJmol^{-1}) refers to the temperature interval from 23 to 83^{o}C, while the other value (E_a = 70.4 kJmol^{-1}) refers to the lower testing temperatures, from 3 to 23^{o}C. These values correspond to different processes that control the v_{pl}. It was proposed that the crack propagation v_{pl} at temperatures above ~ 40^{o}C is associated with aluminium hydride formation (E_a ~ 35 kJmol^{-1}). The decomposition of aluminium hydride within the crack-tip region leads to significantly enhanced local entry of hydrogen, which facilitates the observed increase of v_{pl}, independent of the copper content. The crack propagation v_{pl} at temperatures below ~ 40^{o}C is dependent on the availability of hydrogen generated via the electrochemical process.

CONCLUSIONS

The corrosion resistance of a high strength Al-Zn-Mg-Cu alloywas tested. The alloy was subjected to the standard one-step aging process as well as to a two-step aging process. The measurements of electrical conductivity enabled the estimation of the structural state of the alloy, i.e. the type and the degree of precipitation. The resistance to the localized types of corrosion depends on the presence of different phases developed during the aging process. The value of the corrosion potential depends on the distribution of the alloying elements (Zn, Mg, Cu) in the solid solution and in the precipitated phases such as the $Mg(AlCuZn)_2$ phase. The alloy in the TB state has more positive corrosion potential, compared to the TA state. The polarization measurements have shown that the anodic and cathodic polarization curves of the alloy in the TB state were shifted to the lower values of the current density, and a more positive value of the pitting potential was achieved. The results of electrochemical impedance spectroscopy indicated better corrosion characteristics (higher values of polarization resistance and lower values of double layer capacitance) of the two-stage aged alloy compared to the one-stage aged alloy.

The results obtained with the FM method have a quantitative character. The value of K_{ISCC} is higher, and the v_{pl} is lower for more than one order of magnitude for the two-step aged alloy. The explanation for the processes that take place at the crack tip during SCC of the alloy in the TA and TB states and copper influence is proposed. In the case of real SCC danger in exploitation, the value of the K_{ISCC} should be used in the calculation of the allowed stress, instead of the K_{IC}. For the calculation of the construction work life, the stress corrosion crack growth rate should be applied.Two values of apparent activation energies have been obtained. One value (E_a = 46.6 kJmol^{-1}) refers to the temperature interval from 23 to 83^{o}C, while the other value (E_a = 70.4 kJmol^{-1}) refers to the lower temperatures, from 3 to 23^{o}C. The most likely processes that control the v_{pl} at lower and higher temperatures were suggested. All the results presented enable a deeper insight into different forms of localized corrosion of the aluminium alloys after one- and a two-step aging.

ACKNOWLEDGEMENT

This work was co-financed from the Ministry of Education of the Republic of Serbia (project No. TR 34028 and TR 34018).

REFERENCES

[1] Jones, R. H., Stress-Corrosion Cracking, in Corrosion: Fundamentals, Testing, and Protection, Vol 13A, ASM Handbook, ASM International, 2003, p 346–366
[2] Landolt, D., Corrosion and Surface Chemistry of Metals, Lausanne, Switzerland, 2007.
[3] Brown, B. F., Stress Corrosion Cracking Control Measures, NACE, monograph 156, Ohio, 1977.
[4] Moran, J., Effects of Metallurgical Variables on the Corrosion of Aluminum Alloys, in Corrosion: Fundamentals, Testing, and Protection, Vol 13A, ASM Handbook, ASM International, 2003, pp. 275–278
[5] Fontana, M. G. and Staehle, R.W., Advances in Corrosion Science and Technology, vol. 2, vol. 3 and vol. 7, Plenum Press, New York, 1972, 1973 and 1980 (Russian translation).
[6] Bobby, M., Kannan, P., BALA, S., RAJA, V. S., Stress corrosion cracking (SCC) of aluminium alloys, in Stress corrosion cracking, Theory and practice, Edited by: Raja, V. S. and Shoji, T., Oxford, Cambridge, Philadelphia, New Delhi, 2011, pp. 307-340.
[7] Sinjavskij, V. S., Valjkov, V. D., Kalinin, V. D., Korrozijaizaschitaaljuminijevihsplavov, Moskva, Metalurgija, 1986.
[8] Jegdić, B., "Behavior of Stress Corrosion Crack in a High-Strength Aluminum Alloys Structure", Scientific-Technical Review, LIII (2003) 19-24.
[9] Summerson, T. J. and Sprowls, D. O., Corrosion Behavior of Aluminum Alloys, Vol. III, Conference Proceedings, Aluminum Alloys-Physical and Mechanical Properties, Ed. Starke E. A. and Sanders, T. H., Virginia, June 1986, pp. 1576-1662.
[10] Hatch, J.E., Aluminum: Properties and Physical Metallurgy, American Society for Metals, 1984.
[11] Mondolfo, L. F., Aluminum Alloys: Structure and Properties, Butterworths, 1976.
[12] Burleigh, T. D., "The Postulated Mechanisms for Stress Corrosion Cracking of Aluminum Alloys, A Review of the Literature" 1980-1989, Corrosion, 47 (1991) 89-97.
[13] Andreatta, F., Terryn, H., de Wit, J. H. W., "Corrosion behaviour of different tempers of AA7075 aluminium alloy", ElectrochimicaActa 49 (2004) 2851–2862.